Supplement of Atmos. Chem. Phys., 25, 2967–2978, 2025
https://doi.org/10.5194/acp-25-2967-2025-supplement

Atmospheric Chemistry and Physics
Open Access

Supplement of

Non-biogenic sources are an important but overlooked contributor to aerosol isoprene-derived organosulfates during winter in northern China

Ting Yang et al.

Correspondence to: Yu Xu (xuyu360@sjtu.edu.cn)

Table of Contents

S1. Classification of organosulfates

Organosulfates (OSs) were identified using an UPLC-ESI-QToFMS (Waters, USA) in negative (–) ion mode (Wang et al. 2021a; Yang et al. 2023). The obtained data were processed with a MassLynx v4.1 software to obtain the m/z ratios, formulas, retention times, and peak areas of identified OSs. The identified compounds can be expressed as $C_cH_hO_oN_nS_s$ with a mass tolerance of ± 10 ppm (where c, h, o, n, and s represent the number of carbon, hydrogen, oxygen, nitrogen, and sulfur atoms, respectively). Compounds with oxygen atoms equal to or greater than $4n_S + 3n_N$ (i.e., $n_O/(4n_S + 3n_N) \geq 1$) were tentatively classified as OSs (Cai et al. 2020). The assignments of most OSs were further conducted based on the identification of sulfur-containing fragment ions (e.g., m/z 80, 81, and 96) by MS/MS analysis (Hettiyadura et al. 2015; Ding et al. 2022), which was detailed in our recent publication (Yang et al. 2023). The double bond equivalent value (DBE), indicating the number of rings and double bonds in an organic molecule, can be calculated using the following equation (Han et al. 2023).

$$DBE = 1 + n_C - n_H/2 + n_N/2 \quad (S1)$$

where n_N, n_H, and n_C indicate the numbers of N, H, and C atoms in a molecular formula, respectively.

All identified OSs were classified into five categories, including isoprene-derived (OS_i), monoterpene-derived (OS_m), C_2–C_3 OSs, aromatic OSs and aliphatic OSs (Yang et al. 2023). The list of OS_i was obtained through the following method: (1) molecules with $n_C = 4$ and 5 were selected; (2) C_4 OSs with DBE range of 1–2, $n_O \leq 6$, and $n_H \geq 6$; and (3) C_5 OSs with DBE range of 0–2, $n_O \leq 7$, and $n_H \geq 8$. It should be noted that

$C_7H_9O_7S^-$ was classified as OS_i based on a previous study (Nozière et al. 2010). The detailed workflow was provided in our previous study (Yang et al. 2023).

According to previous laboratory studies, most of OS_m contain 10 carbon atoms, with effective oxygen atoms ($n_{Oeff} = n_O - 2n_N$) exceeding 4, and $2 \leq DBE \leq 4$ (Guo et al. 2022; Ehn et al. 2012; Yan et al. 2016; Jokinen et al. 2014; Boyd et al. 2015; Berndt et al. 2016; Berndt et al. 2018). Additionally, $C_9H_{15}O_6S^-$, $C_7H_{11}O_7S^-$, $C_9H_{14}NO_8S^-$, $C_7H_{11}O_6S^-$, and $C_8H_{13}O_7S^-$were classified into the OS_m category based on previous studies (Yassine et al. 2012; Surratt et al. 2008; Wang et al. 2017). Furthermore, a correlation analysis was conducted between the selected OSs and representative OS_m (e.g., $C_{10}H_{17}O_5S^-$) (Bryant et al. 2021). If a significant correlation ($r > 0.6$ and $P < 0.01$) was found between them, the corresponding OS compound was subsequently classified as OS_m.

The aromaticity equivalent (X_c) describes potential monocyclic and polycyclic aromatic compounds. It has been suggested that OSs with $DBE \geq 2$ and aromaticity equivalent (X_C) ≥ 2.5 can be classified as aromatic OSs (Jiang et al. 2022; Xie et al. 2021; Xie et al. 2020; Ma et al. 2022). The X_C can be calculated using the following equation (Yassine et al. 2014).

$$X_C = [3(DBE - (f_m n_O - f_n n_S)) - 2] / [DBE - (f_m n_O - f_n n_S)] \quad (S2)$$

where the symbols f_n and f_m correspond to the fractions of S and O atoms involved in the π-bond structure of the compound, respectively (Yassine et al. 2014). The negative ion mode exhibits a preferential detection capability for compounds such as carboxylic acids and esters (Ye et al. 2021). Thus, the calculation for Xc of organosulfates can be simplified as the following equation (Ye et al. 2021).

$$X_C = [3(DBE - 0.5(n_O - 4)) - 2] / [DBE - 0.5(n_O - 4)]) \quad (S3)$$

Nonetheless, previous studies have suggested that a DBE value of 2 for OS_m species can be formed via the oxidation of monoterpene by NO_3• or •OH (Yan et al. 2016; Ehn et al. 2014; Trostl et al. 2016). Clearly, it is difficult to completely distinguish aromatic OSs from OS_m based on DBE values. Hence, aromatic OSs with a DBE value of 2 were further screened according to correlation analysis between unidentified aromatic OSs and identified aromatic OSs and OS_m (Yang et al. 2023). The acceptance threshold for the above screening was $r > 0.6$ and $P < 0.01$ (Yang et al. 2023).

The observed OSs with a DBE < 2, such as alkanes and some other unsaturated compounds, were classified as aliphatic OSs (Xie et al. 2020; Tao et al. 2014). However, some aliphatic oxygenated organic molecules were found to have a DBE value of 2 (Wang et al. 2021b). Thus, a correlation analysis was conducted between OSs with DBE = 2 and identified aliphatic species. If a significant correlation ($r > 0.6$ and $P < 0.01$) was found between them, the corresponding OS compound was assigned to aliphatic OSs. Additionally, both of aliphatic and aromatic OSs belonged to the category of anthropogenic OSs (OS_a) (Riva et al. 2016; Riva et al. 2015).

S2. Quantification of OSs

The accurate quantification of OSs is challenging due to the absence of authentic standards. Consequently, the majority of the identified OSs were quantified using surrogate standards (Hettiyadura et al. 2019; Bryant et al. 2021; Wang et al. 2018; Ding et al. 2022). The surrogate standards utilized in this study were as follows. Glycolic acid sulfate (GAS, $C_2H_3O_6S^-$), lactic acid sulfate (LAS, $C_3H_5O_6^-$), limonaketone sulfate ($C_9H_{15}O_6S^-$), and α-pinene sulfate ($C_{10}H_{17}O_5S^-$) were self synthesized according to previous studies (Olson et al. 2011; Wang et al. 2017). Methyl sulfate ($CH_3O_4S^-$, 99%, Macklin), potassium phenyl sulfate ($C_6H_5O_4S^-$, 98%, Tokyo Chemical Industry), and sodium octyl sulfate ($C_8H_{17}O_4S^-$, 95%, Sigma-Aldrich) are commercial standards (Olson et al. 2011; Huang et al. 2018; Wang et al. 2018; Wang et al. 2020). Our previous studies have validated the reliability of these surrogates (Wang et al. 2021a; Yang et al. 2023). In this study, 111 OS were quantified using the aforementioned surrogate standards. It is evident that OSs with similar carbon backbone structures typically exhibit analogous MS responses (Wang et al. 2021a). Consequently, the selection of a surrogate standard for a specific OS was predominantly contingent on the similarity between the carbon chain structures of the targeted OS species and the OS standard (Hettiyadura et al. 2017). Furthermore, the sulfur-containing fragment ions observed in the MS/MS spectra of the standard and targeted OS species have been taken into consideration (Hettiyadura et al. 2019; Bryant et al. 2021). The recoveries of the aforementioned surrogate standards were, in order, 88%, 84%, 94%, 89%, 88%, 87%, and 84%. Additional details on the identification of OS compounds, their classification and quantifacation, and data quality control are available in our recent publications (Yang et al. 2023; Yang et al. 2024). It is crucial to highlight that the OS species quantified in this study should not be interpreted as an exact measurement of OS compounds. Instead, our method represents the optimal approach in the absence of authentic OS standards (Yang et al. 2023; Huang et al. 2023).

S3. Estimation of isoprene emission rate

The isoprene emission rate (I) can be calculated using the following equation (Guenther et al. 1993).

$$I = I_S \times C_L \times C_T \qquad \text{(S4)}$$

where the Is value is defined as the constant at 30°C leaf temperature and 1000 μmol m^{-2} s^{-1} photosynthetically active radiation (PAR). The terms "C_L" and "C_T" denote the factors that influence light and temperature, respectively.

C_L and C_T can be simply estimated as:

$$C_L = \frac{\alpha C_{L1} L}{\sqrt{\alpha^2 L^2 + 1}} \qquad \text{(S5)}$$

$$C_T = \frac{\exp\frac{C_{T1}(T - T_S)}{RT_S T}}{1 + \exp\frac{C_{T2}(T - T_M)}{RT_S T}} \qquad \text{(S6)}$$

where C_{T2} = 230000 J mol^{-1}, T_M = 314 K, R = 8.314 J K^{-1} mol^{-1}, α = 0.0027, T_S = 303 K, C_{L1} = 1.066, and C_{T1} = 95000 J mol^{-1}. T is leaf temperature (K). L denotes PAR in μmol m^{-2} s^{-1} (Guenther et al. 1993). The data on daily mean temperature and solar radiation during the sampling periods were retrieved from the National Meteorological Science Data Center (https://data.cma.cn/). PAR was calculated by solar radiation multiplying photon flux efficacy of 1.86 μmol J^{-1} (Ding et al. 2016). The value of $C_L \times C_T$ was utilized as an indicator to estimate isoprene emission rate (Ding et al. 2016; Guenther et al. 1993).

Table S1. Mean values (± SD) of the major parameters observed in different cities.

Parameter	Southern cities		Northern cities	
	GZ	KM	TY	XA
T (°C)	15.9 ± 3.25	9.63 ± 2.52	-2.56 ± 2.14	1.69 ± 2.24
RH (%)	62.04 ± 21.39	68.25 ± 7.73	42.74 ± 8.78	49.27 ± 17.47
Wind speed (m/s)	3.27 ± 2.07	4.17 ± 1.11	2.44 ± 1.07	6.33 ± 3.36
NO_2 (μg m^{-3})	71.07 ± 26.89	44.01 ± 16.15	61.11 ± 33.72	79.02 ± 26.17
O_3 (μg m^{-3})	34.62 ± 22.76	37.55 ± 16.19	30.07 ± 22.84	24.67 ± 13.35
O_x (μg m^{-3})	105.69 ± 40.9	81.55 ± 20.2	91.19 ± 15.42	103.69 ± 17.13
$C_L \times C_T$	0.16 ± 0.07	0.07 ± 0.03	0.01 ± 0.00	0.02 ± 0.01
SO_2 (μg m^{-3})	15.87 ± 6.29	18.45 ± 5.34	60.36 ± 40.28	31.73 ± 12.13
ALW (μg m^{-3})	19.62 ± 25.35	8.18 ± 6.42	21.18 ± 21.21	51.63 ± 81.74
pH	2.65 ± 0.76	4.06 ± 1.61	5.99 ± 0.92	5.13 ± 0.9
NO_3^- (μg m^{-3})	6.43 ± 3.53	4.83 ± 3.80	14.95 ± 14.27	40.56 ± 31.79
SO_4^{2-} (μg m^{-3})	8.96 ± 6.11	8.09 ± 4.53	14.12 ± 13.66	21.58 ± 17.3
Ca^{2+} (μg m^{-3})	1.01 ± 0.51	2.91 ± 1.07	6.09 ± 1.72	6.69 ± 5.72
Mg^{2+} (μg m^{-3})	0.05 ± 0.02	0.08 ± 0.03	0.34 ± 0.13	0.36 ± 0.36
Nss-K^+ (μg m^{-3})	0.76 ± 0.59	0.53 ± 0.36	1.20 ± 0.98	2.64 ± 1.99
Na^+ (μg m^{-3})	0.17 ± 0.11	0.08 ± 0.07	1.69 ± 0.85	1.59 ± 2.36
NH_4^+ (μg m^{-3})	4.88 ± 2.41	3.78 ± 2.67	12.11 ± 11.66	20.58 ± 17.78
Nss-Cl^- (μg m^{-3})	0.46 ± 0.43	0.74 ± 0.36	6.39 ± 5.55	5.90 ± 3.80
$PM_{2.5}$ (μg m^{-3})	56.41 ± 33.06	47.62 ± 30.50	81.02 ± 65.20	115.33 ± 88.85
Total OS_i (ng m^{-3})	86.65 ± 60.25	61.12 ± 37.75	170.69 ± 68.75	260.32 ± 71.13
Total OS_m (ng m^{-3})	57.81 ± 40.77	58.9 ± 29.70	22.34 ± 7.71	40.09 ± 12.31
Total aromatic OSs (ng m^{-3})	10.31 ± 4.64	7.81 ± 2.25	27.10 ± 17.30	34.75 ± 8.91
Total aliphatic OSs (ng m^{-3})	8.23 ± 3.77	10.41 ± 5.33	14.13 ± 7.91	19.46 ± 8.11
Total C_2-C_3 OSs (ng m^{-3})	25.22 ± 15.09	28.55 ± 16.4	13.43 ± 2.34	25.81 ± 10.76

Table S2. Mean mass concentrations (± SD) of identified OS_i, OS_m, and C_2-C_3 OSs in $PM_{2.5}$ collected in different cities.

Formula $[M-H]^-$	MW (Da)	Southern cities GZ (ng m^{-3})	Southern cities KM (ng m^{-3})	Northern cities TY (ng m^{-3})	Northern cities XA (ng m^{-3})
OS_i					
$C_4H_7O_5S^-$	167.0014	2.7 ± 1.53	2.77 ± 1.71	3.07 ± 0.72	4.74 ± 1.72
$C_4H_6O_5S^-$	165.9936	7.86 ± 4.70	5.97 ± 4.78	29.54± 19.77	23.40 ± 13.74
$C_5H_9O_6S^-$	197.0120	15.94 ± 10.59	11.82 ± 8.42	75.92 ±46.15	71.09 ± 24.18
$C_4H_7O_7S^-$	198.9912	12.63 ± 10.16	10.38 ± 9.11	10.42 ± 8.97	13.50 ± 3.81
$C_5H_{11}O_6S^-$	199.0276	1.69 ± 1.32	2.04 ± 1.52	2.43 ± 0.85	1.60 ± 0.48
$C_5H_7O_7S^-$	210.9912	6.03 ± 8.30	3.74 ± 2.51	7.65 ± 3.92	10.93 ± 6.24
$C_5H_9O_7S^-$	213.0069	10.07 ± 8.88	6.21 ± 4.34	24.49 ±12.27	104.72 ± 44.75
$C_5H_{11}O_7S^-$	215.0225	3.22 ± 3.36	2.83 ± 1.76	0.73 ± 0.19	1.93 ± 0.62
$C_7H_9O_7S^-$	237.0069	4.74 ± 3.69	1.56 ± 1.27	1.57 ± 0.96	3.35 ± 1.40
$C_5H_8NO_{10}S^-$	273.9869	0.25 ± 0.04	0.29 ± 0.05	0.32 ± 0.07	0.29 ± 0.12
$C_5H_7O_8S^-$	226.9862	10.18 ± 7.12	3.80 ± 2.90	2.25 ± 1.72	5.33 ± 3.26
$C_4H_8NO_7S^-$	243.9763	0.79 ± 0.35	0.74 ± 0.40	1.34 ± 0.53	3.91 ± 1.97
$C_4H_7O_8S^-$	214.9862	0.87 ± 0.41	1.76 ± 1.63	3.62 ± 3.96	1.28 ± 0.78
$C_4H_5O_7S^-$	196.9756	2.40 ± 1.28	1.58 ± 0.70	1.33 ± 0.44	2.36 ± 1.90
$C_4H_6NO_9S^-$	243.9763	0.28 ± 0.06	0.28 ± 0.04	0.24 ± 0.04	0.27 ± 0.06
$C_5H_9O_8S^-$	229.0018	3.07 ± 1.90	3.71 ± 2.49	3.62 ± 2.46	6.86 ± 2.70
$C_5H_{10}NO_9S^-$	260.0076	0.18 ± 0.00	0.23 ± 0.03	0.19 ± 0.01	0.18 ± 0.00
$C_5H_8NO_7S^-$	226.0021	3.74 ± 2.81	1.41 ± 1.00	1.98 ± 1.43	4.59 ± 2.62
OS_m					
$C_7H_{11}O_6S^-$	223.0276	9.51 ± 6.01	6.48 ± 4.59	7.07 ± 3.40	7.67 ± 2.80
$C_7H_{11}O_7S^-$	239.0225	10.23 ± 9.22	5.65 ± 4.62	4.49 ± 2.18	6.68 ± 2.86
$C_9H_{15}O_6S^-$	251.0589	0.23 ± 0.06	0.68 ± 0.24	0.25 ± 0.05	0.41 ± 0.13
$C_8H_{13}O_7S^-$	253.0382	2.05 ± 1.65	0.51 ± 0.13	2.59 ± 1.96	2.56 ± 0.81
$C_{10}H_{15}O_7S^-$	279.0538	8.23 ± 8.25	3.96 ± 3.05	1.87 ± 0.52	3.54 ± 1.88
$C_{10}H_{16}NO_7S^-$	294.0647	18.26 ± 14.43	15.88 ± 11.68	2.62 ± 0.82	6.81 ± 3.17
$C_9H_{14}NO_8S^-$	296.0440	4.5 8 ± 2.19	20.15 ± 8.81	1.62 ± 0.80	8.92 ± 3.59
$C_{10}H_{16}NO_{10}S^-$	342.0495	1.18 ± 0.52	3.50 ± 2.03	0.71 ± 0.37	1.73 ± 1.67
$C_{10}H_{15}O_5S^-$	247.0640	2.45 ± 2.54	0.58 ± 0.37	0.24 ± 0.02	0.55 ± 0.17
$C_{10}H_{15}O_6S^-$	263.0589	0.26 ± 0.09	0.46 ± 0.17	0.16 ± 0.03	0.37 ± 0.09
$C_{10}H_{17}O_6S^-$	265.0746	0.11 ± 0.01	0.15 ± 0.02	0.11 ± 0.02	0.11 ± 0.01
$C_{10}H_{17}O_8S^-$	297.0644	0.17 ± 0.08	0.19 ± 0.04	0.16 ± 0.04	0.22 ± 0.08
$C_{10}H_{15}O_8S^-$	295.0488	0.13 ± 0.04	0.18 ± 0.04	0.10 ± 0.01	0.12 ± 0.02
$C_{10}H_{17}NO_9S^-$	326.0546	0.10 ± 0.00	0.13 ± 0.02	0.13 ± 0.02	0.11 ± 0.01
$C_9H_{11}O_8S^-$	279.0175	0.23 ± 0.09	0.28 ± 0.07	0.12 ± 0.01	0.17 ± 0.04
C_2-C_3 OSs					
$C_3H_5O_4S^-$	136.9909	1.92 ± 0.64	2.03 ± 0.51	2.52 ± 0.61	3.16 ± 1.04
$C_2H_3O_5S^-$	138.9701	1.39 ± 0.28	1.53 ± 0.26	1.16 ± 0.08	1.16 ± 0.14
$C_3H_5O_5S^-$	152.9858	5.07 ± 2.89	4.12 ± 1.43	2.82 ± 0.55	4.72 ± 1.73
$C_2H_3O_6S^-$	154.9650	8.45 ± 5.52	9.8 ± 6.65	2.25 ± 0.35	5.36 ± 1.94
$C_3H_7O_5S^-$	155.0014	2.31 ± 0.99	3.84 ± 1.81	2.77 ± 1.61	5.47 ± 4.61
$C_3H_5O_6S^-$	168.9807	6.07 ± 5.22	7.24 ± 6.38	1.91 ± 0.69	5.95 ± 2.49

Table S3. The mean mass concentrations (± SD) of identified anthropogenic OSs in $PM_{2.5}$ collected in different cities.

Formula [M-H]⁻	MW(Da)	Southern cities GZ (ng m^{-3})	Southern cities KM (ng m^{-3})	Northern cities TY (ng m^{-3})	Northern cities XA (ng m^{-3})
Aliphatic OSs					
$C_{12}H_{21}O_7S^-$	309.1008	0.07 ± 0.04	0.04 ± 0.03	0.04 ± 0.04	0.05 ± 0.05
$C_8H_{17}O_4S^-$	210.0926	0.07 ± 0.05	0.45 ± 0.36	0.49 ± 0.21	0.49 ± 0.16
$C_{14}H_{29}O_5S^-$	309.1736	0.15 ± 0.11	0.21 ± 0.07	0.53 ± 0.55	0.46 ± 0.43
$C_7H_{15}O_4S^-$	195.0691	0.12 ± 0.24	0.25 ± 0.18	1.18 ± 0.56	0.87 ± 0.41
$C_7H_{15}O_5S^-$	211.064	0.05 ± 0.04	0.06 ± 0.03	0.06 ± 0.02	0.15 ± 0.10
$C_9H_{19}O_4S^-$	223.1004	0.26 ± 0.11	0.67 ± 0.65	0.90 ± 0.57	1.2 6± 0.74
$C_{10}H_{21}O_4S^-$	237.1161	0.27 ± 0.11	0.44 ± 0.90	0.82 ± 0.34	1.01 ± 0.97
$C_7H_{13}O_5S^-$	209.0484	0.20 ± 0.08	0.16 ± 0.09	0.36 ± 0.10	0.67 ± 0.13
$C_9H_{17}O_5S^-$	237.0797	0.09 ± 0.09	0.09 ± 0.04	0.56 ± 0.26	0.46 ± 0.26
$C_{10}H_{19}O_5S^-$	251.0953	0.82 ± 0.42	0.18 ± 0.12	0.31 ± 0.11	0.39 ± 0.15
$C_9H_{17}O_7S^-$	269.0695	0.18 ± 0.23	0.06 ± 0.06	0.02 ± 0.01	0.09 ± 0.06
$C_{12}H_{23}O_5S^-$	279.1266	0.05 ± 0.04	0.03 ± 0.01	0.08 ± 0.06	0.11 ± 0.04
$C_9H_{17}O_4S^-$	221.0848	0.23 ± 0.39	0.57 ± 0.60	0.79 ± 0.46	1.20 ± 0.40
$C_9H_{17}O_6S^-$	253.0746	0.30 ± 0.32	0.21 ± 0.15	0.13 ± 0.06	0.31 ± 0.26
$C_{13}H_{25}O_5S^-$	293.1423	0.43 ± 0.32	0.26 ± 0.18	0.56 ± 0.32	0.88 ± 0.34
$C_{14}H_{27}O_5S^-$	307.1579	0.49 ± 0.31	0.32 ± 0.24	0.62 ± 0.41	0.88 ± 0.38
$C_{13}H_{25}O_6S^-$	309.1372	0.04 ± 0.04	0.04 ± 0.03	0.09 ± 0.07	0.16 ± 0.14
$C_{14}H_{27}O_6S^-$	323.1528	0.09 ± 0.08	0.13 ± 0.07	0.23 ± 0.21	0.43 ± 0.36
$C_{16}H_{31}O_5S^-$	335.1892	0.10 ± 0.11	0.17 ± 0.15	0.42 ± 0.43	0.44 ± 0.39
$C_{17}H_{33}O_5S^-$	363.2205	0.04 ± 0.01	0.23 ± 0.11	0.13 ± 0.10	0.16 ± 0.10
$C_{16}H_{31}O_6S^-$	351.1841	1.43 ± 0.92	2.64 ± 1.55	2.75 ± 2.39	4.87 ± 3.81
$C_{18}H_{35}O_5S^-$	363.2205	0.06 ± 0.06	0.06 ± 0.04	0.19 ± 0.19	0.31 ± 0.26
$C_{21}H_{41}O_5S^-$	405.2675	0.01 ± 0.01	0.01 ± 0.01	0.02 ± 0.03	0.02 ± 0.01
$C_8H_{15}O_5S^-$	223.0640	0.11 ± 0.05	0.18 ± 0.14	0.24 ± 0.10	0.29 ± 0.12
$C_7H_{13}O_6S^-$	225.0433	0.18 ± 0.18	0.12 ± 0.11	0.16 ± 0.16	0.30 ± 0.09
$C_8H_{15}O_6S^-$	239.0589	0.26 ± 0.17	0.54 ± 0.28	0.26 ± 0.10	0.46 ± 0.31
$C_{11}H_{21}O_5S^-$	265.1110	0.15 ± 0.06	0.14 ± 0.08	0.29 ± 0.14	0.49 ± 0.22
$C_{10}H_{19}O_6S^-$	267.0902	0.11 ± 0.08	0.12 ± 0.06	0.20 ± 0.08	0.21 ± 0.14
$C_7H_{13}O_9S^-$	273.0280	0.08 ± 0.07	0.30 ± 0.33	0.55 ± 0.29	0.38 ± 0.31
$C_{15}H_{29}O_5S^-$	321.1736	0.46 ± 0.40	0.27 ± 0.28	0.33 ± 0.38	0.47 ± 0.11
$C_{10}H_{17}O_6S^-$	265.0746	0.05 ± 0.02	0.06 ± 0.04	0.05 ± 0.03	0.11 ± 0.06
$C_9H_{15}O_5S^-$	235.0640	0.34 ± 0.24	0.41 ± 0.12	0.10 ± 0.06	0.15 ± 0.06
$C_{10}H_{17}O_5S^-$	249.0797	0.13 ± 0.07	0.55 ± 0.32	0.11 ± 0.04	0.28 ± 0.14
$C_9H_{15}O_6S^-$	251.0589	0.30 ± 0.29	0.19 ± 0.12	0.41 ± 0.27	0.43 ± 0.15
$C_{11}H_{19}O_6S^-$	279.0902	0.03 ± 0.02	0.03 ± 0.02	0.07 ± 0.04	0.10 ± 0.04
$C_8H_{13}O_6S^-$	237.0433	0.13 ± 0.06	0.09 ± 0.05	0.04 ± 0.01	0.08 ± 0.03
$C_9H_{15}O_7S^-$	267.0538	0.33 ± 0.39	0.10 ± 0.08	0.01 ± 0.01	0.05 ± 0.03
Aromatic OSs					
$C_9H_9O_4S^-$	213.0222	1.88 ± 1.62	0.91 ± 0.50	6.22 ± 3.54	18.88 ± 7.88
$C_6H_5O_4S^-$	172.9909	0.24 ± 0.08	0.27 ± 0.22	1.42 ± 1.02	0.72 ± 0.33
$C_7H_7O_4S^-$	187.0065	0.24 ± 0.18	0.25 ± 0.07	1.31 ± 0.55	0.56 ± 0.22
$C_{11}H_{19}O_{11}S^-$	359.0648	0.15 ± 0.05	0.16 ± 0.05	0.18 ± 0.07	0.38 ± 0.12
$C_{10}H_{17}O_{12}S^-$	361.0441	0.09 ± 0.01	0.11 ± 0.02	0.10 ± 0.01	0.10 ± 0.01
$C_7H_{11}O_{10}S^-$	287.0073	0.14 ± 0.05	0.14 ± 0.04	0.10 ± 0.02	0.12 ± 0.04
$C_8H_{13}O_9S^-$	285.0280	0.34 ± 0.24	0.23 ± 0.12	0.89 ± 0.75	0.44 ± 0.18
$C_8H_{13}O_{10}S^-$	301.0229	0.16 ± 0.08	0.15 ± 0.06	0.13 ± 0.04	0.17 ± 0.06
$C_{11}H_{17}O_{11}S^-$	357.0492	0.16 ± 0.16	0.21 ± 0.08	0.20 ± 0.10	0.12 ± 0.02
$C_9H_{11}O_{13}S^-$	358.9920	0.11 ± 0.03	0.12 ± 0.02	0.11 ± 0.02	0.12 ± 0.05
$C_8H_{12}NO_{11}S^-$	330.0131	0.20 ± 0.13	0.12 ± 0.03	0.14 ± 0.06	0.20 ± 0.12
$C_7H_7SO_4S^-$	218.9786	0.11 ± 0.04	0.14 ± 0.02	0.29 ± 0.08	0.19 ± 0.10
$C_8H_7O_5S^-$	215.0014	0.57 ± 0.30	0.33 ± 0.18	4.04 ± 3.58	1.77 ± 1.36

$C_8H_7NO_5S^-$	229.0045	0.61 ± 0.35	0.68 ± 0.41	0.87 ± 0.52	1.13 ± 0.47
$C_9H_9O_6S^-$	245.0120	0.29 ± 0.33	0.20 ± 0.06	0.70 ± 0.45	0.82 ± 0.41
$C_8H_7O_4S^-$	199.0065	0.73 ± 0.47	0.28 ± 0.13	2.51 ± 2.10	2.13 ± 0.79
$C_9H_7O_7S^-$	258.9912	0.54 ± 0.48	0.12 ± 0.03	0.35 ± 0.26	0.69 ± 1.34
$C_8H_5O_6S^-$	228.9807	0.38 ± 0.27	0.14 ± 0.03	0.58 ± 0.50	0.67 ± 0.91
$C_9H_7O_6S^-$	242.9963	0.48 ± 0.27	0.28 ± 0.13	1.61 ± 1.47	0.87 ± 0.73
$C_9H_3O_{11}S^-$	318.9396	0.08 ± 0.01	0.10 ± 0.01	0.09 ± 0.01	0.08 ± 0.00
$C_{10}H_5O_{12}S^-$	348.9502	0.08 ± 0.00	0.10 ± 0.01	0.08 ± 0.00	0.08 ± 0.01
$C_{34}H_{49}O_5S^-$	569.3301	0.11 ± 0.04	0.23 ± 0.20	0.57 ± 0.36	0.38 ± 0.26
$C_{43}H_{63}O_5S^-$	691.4396	0.33 ± 0.41	0.52 ± 0.34	0.11 ± 0.03	0.08 ± 0.01
$C_7H_{11}O_9S^-$	271.0124	0.27 ± 0.20	0.23 ± 0.12	0.17 ± 0.07	0.19 ± 0.08
$C_{10}H_7O_{11}S^-$	334.9709	0.08 ± 0.01	0.10 ± 0.01	0.08 ± 0.01	0.08 ± 0.01
$C_{10}H_5O_{11}S^-$	332.9553	0.08 ± 0.00	0.10 ± 0.01	0.09 ± 0.01	0.08 ± 0.00
$C_{10}H_5O_{10}S^-$	316.9603	0.07 ±0.00	0.09 ± 0.01	0.08 ± 0.00	0.07± 0.00
$C_{12}H_7O_{13}S^-$	390.9607	0.08 ± 0.00	0.10 ± 0.01	0.08 ± 0.00	0.08 ± 0.00
$C_7H_5O_5S^-$	200.9858	0.84 ± 0.55	0.42 ± 0.36	3.18 ± 3.76	2.12 ± 2.18
$C_{18}H_{13}O_6S^-$	357.0433	0.11 ± 0.08	0.15 ± 0.05	0.13 ± 0.03	0.11 ± 0.02
$C_{23}H_{19}O_7S^-$	439.0851	0.22 ± 0.14	0.27 ± 0.15	0.14 ± 0.03	0.22 ± 0.11
$C_{25}H_{21}O_7S^-$	465.1008	0.08 ± 0.00	0.11 ± 0.02	0.08 ± 0.00	0.08 ± 0.00
$C_{24}H_{17}O_4S^-$	401.0848	0.38 ± 0.13	0.36 ± 0.14	0.40 ± 0.16	0.90 ± 0.25
$C_{27}H_{21}O_7S^-$	489.1008	0.11 ± 0.03	0.13 ± 0.04	0.10 ± 0.03	0.13 ± 0.03

[a]All aliphatic and aromatic OSs and other anthropogenic OSs were collectively referred to as anthropogenic OSs (OS_a).

Table S4. Mean mass concentrations of various OSs in $PM_{2.5}$ at different locations.

	Sampling site	Period	Season	OS_i (ng m^{-3})	OS_m (ng m^{-3})	C_2-C_3 (ng m^{-3})	OS_a (ng m^{-3})	Total (ng m^{-3})	Reference
Urban site	Atlanta, GA, USA	2014	Summer	1122.98	67.9	58.5	-	1249.38	(Hettiyadura et al. 2019)
	Tianjing, China	2019	Winter	400.00	-	-	-	400.00	(Ding et al. 2022)
	Lahore, Pakistan	2007	Winter	3.80	-	-	2.02	5.82	(Kundu et al. 2013)
	Hong Kong, China	2017	Winter	97.96	17.26	-	-	115.22	(Wang et al. 2022)
	Guangzhou, China	2017	Winter	88.03	20.96	-	-	108.99	
	Xian, China	2014	Winter	-	0.14	77.30	-	77.44	(Huang et al. 2018)
	Shanghai, China	2021	Summer	85.38	30.61	19.31	23.38	158.68	(Yang et al. 2023)
	Urumqi, China	2018	Winter	62.21	23.33	41.85	168.54	295.93	(Yang et al. 2024)
Suburban site	Zion, Illinois, USA	2013	Spring	121.10	8.70	-		129.80	(Hughes et al. 2021)
Rural site	Look Rock, TN, USA	2013	Summer	1256.75	-	-	-	1256.75	(Budisulistiorini et al. 2015)
	Centreville, AL, USA	2013	Summer	15.40	-	20.83	1.16	37.39	(Hettiyadura et al. 2017)
	Yorkville, GA, USA	2010	Summer	115.11	-	-	-	115.11	(Lin et al. 2013)
	Copenhagen, Denmark	2011	Summer	11.31	0.87	-	-	12.18	(Nguyen et al. 2014)
	National Park, CO, USA	2016	Summer	19.00	-	-	-	-	(Chen et al. 2021)
	Seashore, CA, USA	2016	Summer	22.00	-	-	-	-	
Rural site	Melpitz, Germany	2013	Winter	11.12	49.33	-	32.83	93.28	(Glasius et al. 2018)
	Vavihill, Sweden	2013	Winter	2.75	6.39	-	4.15	13.29	
	Birkenes, Norway	2013	Winter	2.28	6.39	-	2.16	10.83	
Coastal site	The Yellow Sea and Bohai Sea	2019	Summer	22.98	7.53	12.7	-	43.21	(Wang et al. 2023)
Urban site	Guangzhou, China	2017	Winter	86.65	57.81	25.22	18.54	188.22	In this study
	Kunming, China			61.12	58.9	28.55	18.22	166.79	
	Taiyuan, China			170.69	22.34	13.43	41.23	247.69	
	Xi'an, China			260.32	40.09	25.81	54.21	380.43	

Table S5. Relative signal intensity of identified OS_a in different smoke particle samples. The relative signal intensity refers to the percentage of the target OS signal intensity in the total signal intensity of the OS group to which the target OS belongs.

Formula $[M-H]^-$	Rice straw	Pine branch	Coal combustion	Gasoline vehicle	Diesel vehicle
Aliphatic OSs					
$C_8H_{17}O_4S^-$	2.91	0.09	11.23	1.62	0.86
$C_7H_{15}O_4S^-$	4.87	34.02	17.24	1.02	2.90
$C_9H_{19}O_4S^-$	2.92	3.27	2.57	3.81	1.21
$C_{10}H_{21}O_4S^-$	0.40	0.00	0.02	2.86	0.53
$C_9H_{17}O_4S^-$	3.80	0.09	7.35	7.59	59.32
$C_{14}H_{29}O_5S^-$	4.44	0.02	0.00	3.52	0.48
$C_7H_{15}O_5S^-$	0.98	1.02	2.08	0.30	0.47
$C_7H_{13}O_5S^-$	3.40	14.52	1.50	28.70	3.40
$C_9H_{17}O_5S^-$	1.76	3.55	1.27	0.48	0.59
$C_{10}H_{19}O_5S^-$	5.33	0.88	0.31	1.41	0.68
$C_{12}H_{23}O_5S^-$	0.66	1.22	0.02	1.34	1.72
$C_{13}H_{25}O_5S^-$	0.25	0.69	0.12	6.11	3.13
$C_{14}H_{27}O_5S^-$	0.29	2.12	0.00	0.70	0.64
$C_{16}H_{31}O_5S^-$	0.23	0.00	0.00	1.15	6.03
$C_{17}H_{33}O_5S^-$	16.49	7.62	0.17	0.68	0.49
$C_{18}H_{35}O_5S^-$	10.70	0.20	0.02	1.39	0.00
$C_{21}H_{41}O_5S^-$	3.44	0.01	0.02	0.20	0.00
$C_8H_{15}O_5S^-$	0.23	4.09	0.17	0.27	0.24
$C_{11}H_{21}O_5S^-$	0.07	0.48	0.05	0.62	0.28
$C_{15}H_{29}O_5S^-$	1.58	4.10	0.00	1.53	0.00
$C_9H_{15}O_5S^-$	0.68	2.59	0.82	1.98	1.69
$C_{10}H_{17}O_6S^-$	2.91	3.22	0.24	0.47	1.23
$C_9H_{17}O_6S^-$	1.77	2.84	0.11	0.98	0.72
$C_{13}H_{25}O_6S^-$	0.23	0.03	0.36	0.16	2.89
$C_{14}H_{27}O_6S^-$	0.17	0.00	0.24	1.08	5.60
$C_{16}H_{31}O_6S^-$	16.03	0.00	0.24	23.34	0.07
$C_7H_{13}O_6S^-$	0.35	2.65	0.08	0.41	0.21
$C_8H_{15}O_6S^-$	1.97	1.70	0.54	1.95	1.52
$C_{10}H_{19}O_6S^-$	3.47	0.97	47.71	0.44	1.00
$C_{10}H_{17}O6S^-$	0.47	0.55	0.08	0.07	0.03
$C_9H_{15}O_6S^-$	0.16	1.20	0.33	1.08	0.93
$C_{11}H_{19}O_6S^-$	0.51	0.61	1.61	0.27	0.22
$C_{12}H_{21}O_6S^-$	0.10	0.00	0.00	0.02	0.03
$C_{14}H_{25}O_6S^-$	1.25	0.16	0.87	0.14	0.03
$C_8H_{13}O_6S^-$	0.51	0.89	1.41	0.87	0.28
$C_{12}H_{21}O_7S^-$	1.89	0.01	0.23	0.42	0.04
$C_9H_{17}O_7S^-$	2.18	0.47	0.69	0.36	0.33
$C_9H_{15}O_7S^-$	0.03	4.10	0.09	0.52	0.09
$C_7H_{13}O_9S^-$	0.43	0.03	0.16	0.04	0.06
$C_{26}H_{51}O_{12}S^-$	0.18	0.00	0.00	0.10	0.00
$C_{24}H_{51}N_2O_{13}S^-$	0.00	0.00	0.04	0.00	0.06
Aromatic OSs					
$C_{24}H_{17}O_4S^-$	4.88	0.21	0.08	28.12	9.48
$C_6H_5O_4S^-$	0.50	0.79	3.16	0.10	4.92

$C_7H_7O_4S^-$	1.65	0.95	12.12	1.37	14.60
$C_8H_7O_4S^-$	0.43	0.65	1.11	1.16	49.85
$C_9H_9O_4S^-$	75.53	25.38	71.45	1.80	86.58
$C_{34}H_{49}O_5S^-$	0.22	0.00	0.00	0.12	0.00
$C_{43}H_{63}O_5S^-$	0.05	0.22	0.00	0.00	0.17
$C_7H_5O_5S^-$	0.26	1.00	0.10	0.77	0.37
$C_8H_7NO_5S^-$	1.12	12.38	2.73	26.95	6.28
$C_8H_7O_5S^-$	1.67	2.04	2.32	0.86	9.55
$C_{18}H_{13}O_6S^-$	0.02	1.59	0.33	0.09	0.23
$C_8H_5O_6S^-$	0.25	0.09	0.15	0.11	0.83
$C_9H_7O_6S^-$	0.78	13.07	0.67	0.35	2.37
$C_9H_9O_6S^-$	1.67	5.31	0.86	0.39	6.95
$C_{23}H_{19}O_7S^-$	0.01	7.11	0.26	0.62	8.85
$C_{25}H_{21}O_7S^-$	0.02	0.10	0.01	0.09	0.01
$C_{27}H_{21}O_7S^-$	1.43	2.59	2.66	1.80	3.82
$C_9H_7O_7S^-$	0.06	0.09	0.02	0.12	0.70
$C_7H_{11}O_9S^-$	0.07	0.54	0.05	0.47	0.24
$C_8H_{13}O_9S^-$	0.94	4.31	0.26	0.60	0.77
$C_{10}H_5O_{10}S^-$	0.00	0.00	0.00	0.00	0.00
$C_7H_{11}O_{10}S^-$	0.00	0.37	0.00	0.09	0.01
$C_8H_{13}O_{10}S^-$	0.04	0.61	0.06	0.16	0.38
$C_{10}H_5O_{11}S^-$	0.00	0.09	0.01	0.00	0.00
$C_{10}H_7O_{11}S^-$	0.03	0.12	0.14	0.01	0.25
$C_{11}H_{17}O_{11}S^-$	0.18	1.68	0.38	0.70	2.71
$C_{11}H_{19}O_{11}S^-$	3.13	14.58	0.22	4.46	0.37
$C_{12}H_{21}N_2O_{11}S^-$	4.88	0.21	0.17	28.12	9.48
$C_8H_{12}NO_{11}S^-$	0.10	2.37	0.59	0.15	0.00
$C_9H1_3O_{11}S^-$	0.06	1.55	0.04	0.17	0.84
$C_9H_3O_{11}S^-$	0.02	0.01	0.00	0.19	0.07
$C_{10}H_{17}O_{12}S^-$	0.00	0.00	0.07	0.01	0.07
$C_{10}H_5O_{12}S^-$	0.01	0.01	0.01	0.04	0.00

Figure S1.

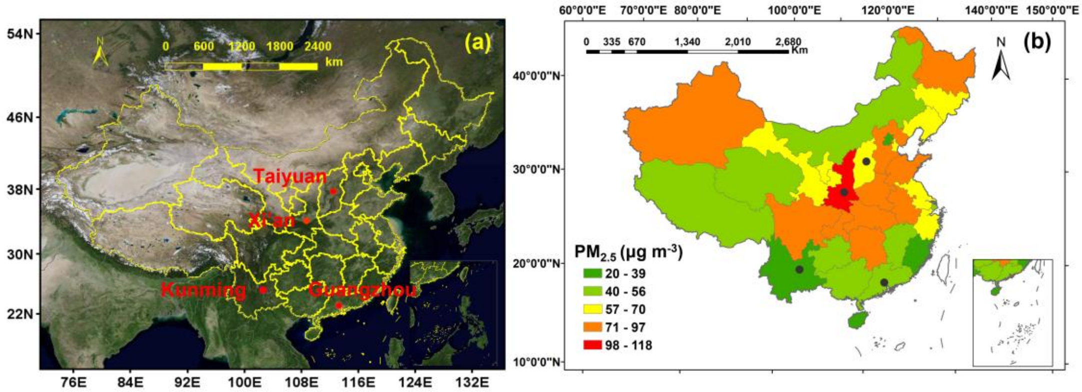

Figure S1. The locations of the sampling sites showing (a) the vegetation coverage in China and (b) the $PM_{2.5}$ pollution situation during winter. The map was derived from ©MeteoInfoMap (version 3.6.2) (Chinese Academy of Meteorological Sciences, China). The figure may contain a territory that is disputed according to the United Nations.

Figure S2.

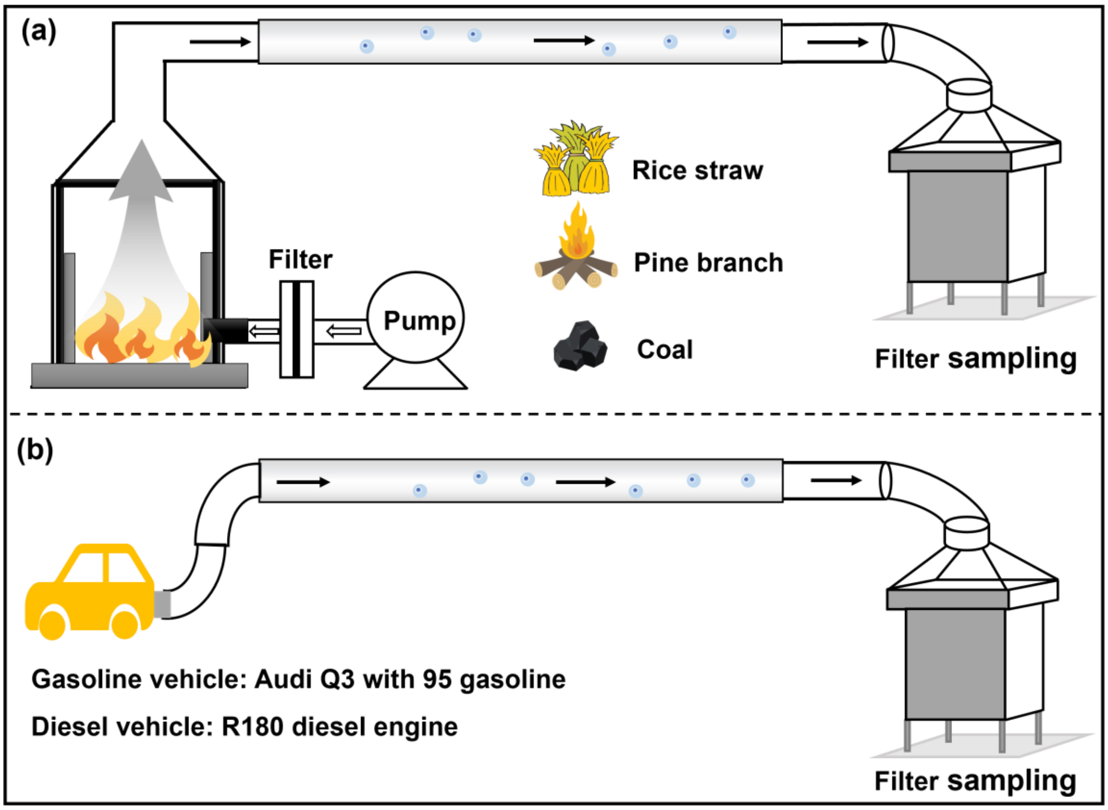

Figure S2. Schematic showing the collections of smoke particles ($PM_{2.5}$) derived from the combustion of (a) rice straw, pine branch, and coal. The samples were collected through a combustion furnace (Tang et al. 2020) pumped with filtered ambient air (particulate matter is removed). The collection method of smoke particles (TSP) derived from liquid fuel combustion was shown in panel (b). The gasoline vehicle was the Audi Q3, while the particles released from diesel combustion were derived from the R180 diesel engine.

Figure S3.

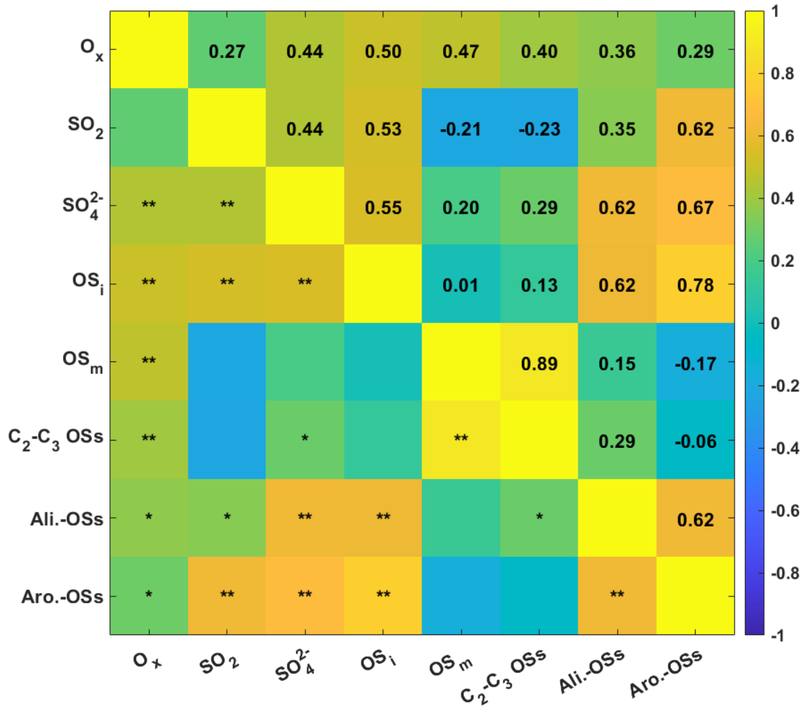

Figure S3. Diagrams presenting Pearson correlations among the concentrations of O_x, SO_2, SO_4^{2-}, and the different OSs (using data from four cities). The numbers in the matrix refer to the correlation coefficients (*r*). Symbols * and ** indicate $P < 0.05$ and $P < 0.01$, respectively.

Figure S4.

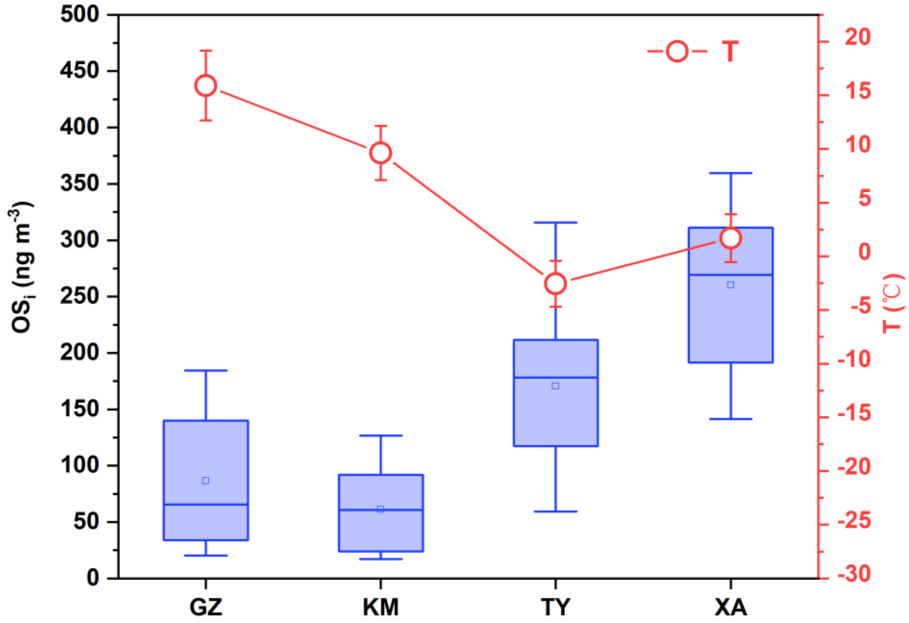

Figure S4. Spatial variation of OS_i concentration and temperature (T).

Figure S5.

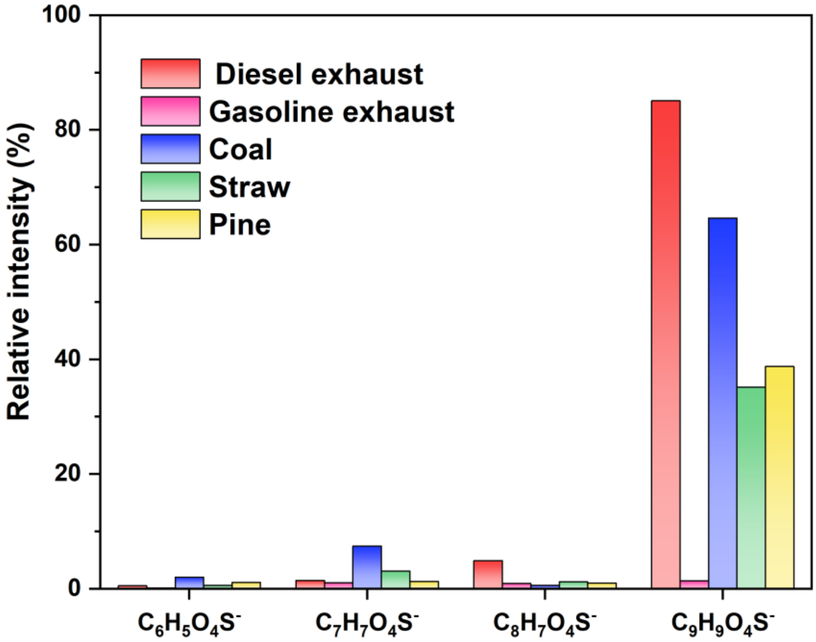

Figure S5. Mean relative signal intensities of typical aromatic OSs (i.e., $C_6H_5O_4S^-$, $C_7H_7O_4S^-$, $C_8H_7O_4S^-$, and $C_9H_9O_4S^-$) in different smoke particle samples. The relative signal intensity refers to the percentage of the target OS signal intensity in the total signal intensity of the OS group to which the target OS belongs.

Figure S6.

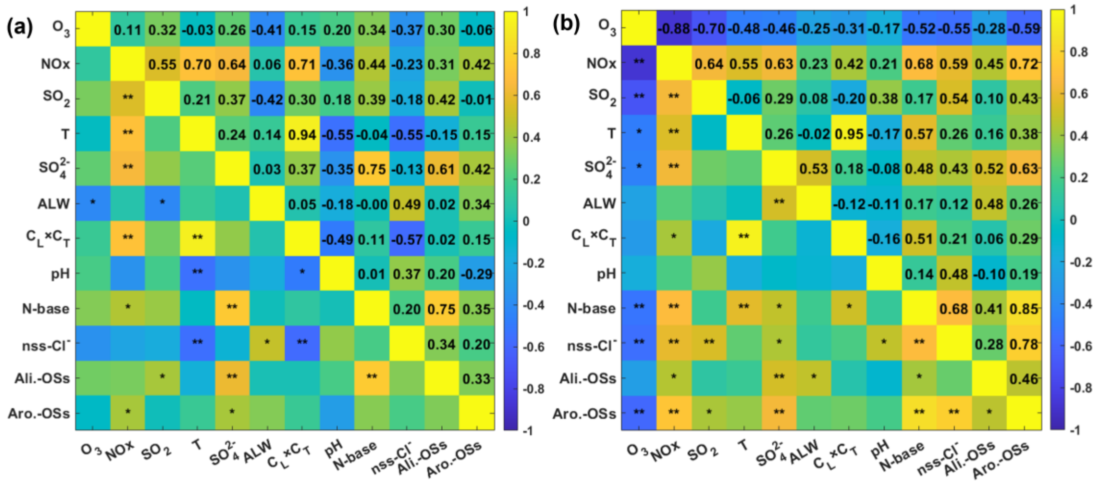

Figure S6. Diagrams presenting Pearson correlations among different OSs and important parameters for the cases in (a) southern cities and (b) northern cities. The numbers in the matrix refer to the correlation coefficients (r). Symbols * and ** indicate $P < 0.05$ and $P < 0.01$, respectively.

Figure S7.

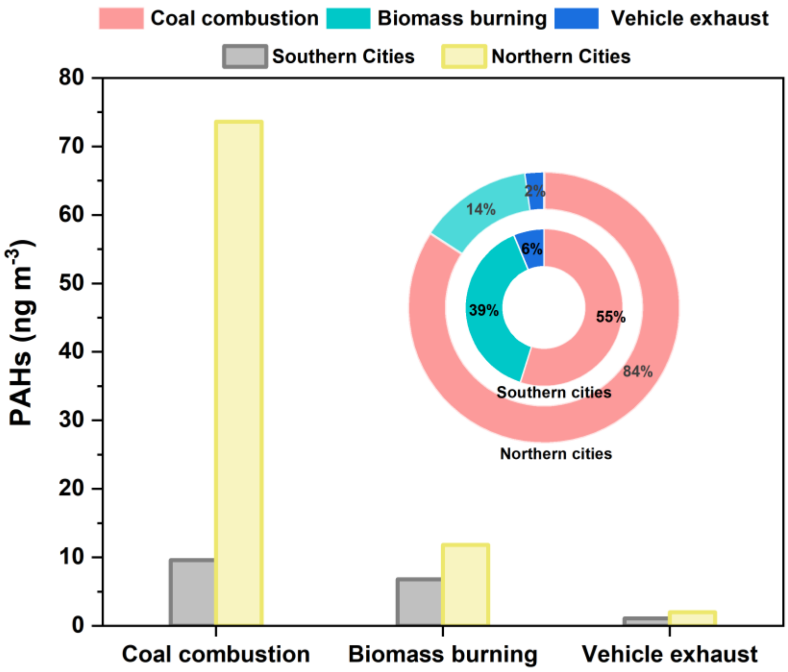

Figure S7. Variations in the concentration and percentage of polyaromatic hydrocarbons (PAHs) emitted from coal combustion, biomass burning, and vehicle exhaust in southern and northern cities. The data were derived from a previous study (Yu et al. 2020).

Figure S8.

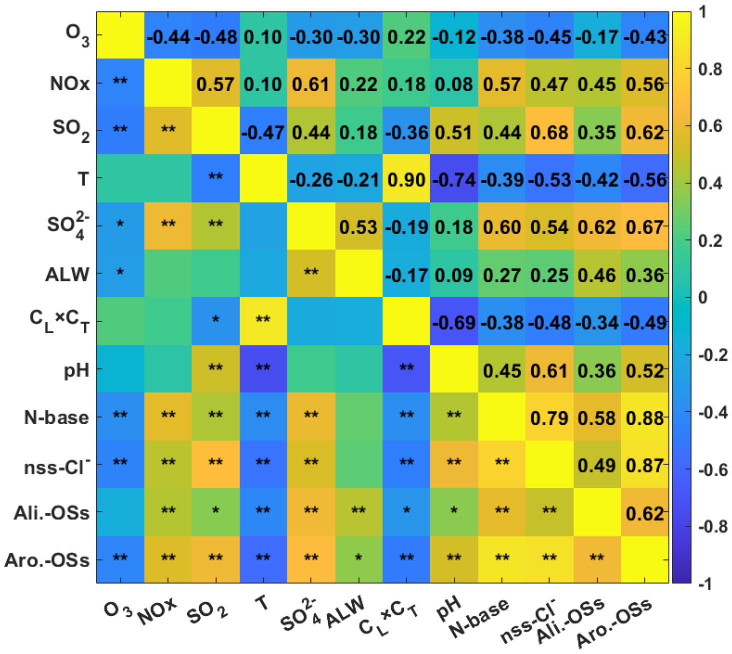

Figure S8. Diagrams presenting Pearson correlations among the different OSs and important parameters (using data from four cities). The numbers in the matrix refer to the correlation coefficients (*r*). Symbols * and ** indicate $P < 0.05$ and $P < 0.01$, respectively.

References

Berndt, T., Mentler, B., Scholz, W., Fischer, L., Herrmann, H., Kulmala, M., and Hansel, A.: Accretion Product Formation from Ozonolysis and OH Radical Reaction of alpha-Pinene: Mechanistic Insight and the Influence of Isoprene and Ethylene, Environ. Sci. Technol., 52, 11069-11077, 10.1021/acs.est.8b02210, 2018.

Berndt, T., Richters, S., Jokinen, T., Hyttinen, N., Kurten, T., Otkjaer, R. V., Kjaergaard, H. G., Stratmann, F., Herrmann, H., Sipila, M., Kulmala, M., and Ehn, M.: Hydroxyl radical-induced formation of highly oxidized organic compounds, Nat. Commun., 7, 13677, 10.1038/ncomms13677, 2016.

Boyd, C. M., Sanchez, J., Xu, L., Eugene, A. J., Nah, T., Tuet, W. Y., Guzman, M. I., and Ng, N. L.: Secondary organic aerosol formation from the β-pinene+NO₃ system: effect of humidity and peroxy radical fate, Atmos. Chem. Phys., 15, 7497-7522, 10.5194/acp-15-7497-2015, 2015.

Bryant, D. J., Elzein, A., Newland, M., White, E., Swift, S., Watkins, A., Deng, W., Song, W., Wang, S., Zhang, Y., Wang, X., Rickard, A. R., and Hamilton, J. F.: Importance of Oxidants and Temperature in the Formation of Biogenic Organosulfates and Nitrooxy Organosulfates, ACS Earth Space Chem., 5, 2291-2306, 10.1021/acsearthspacechem.1c00204, 2021.

Budisulistiorini, S. H., Li, X., Bairai, S. T., Renfro, J., Liu, Y., Liu, Y. J., McKinney, K. A., Martin, S. T., McNeill, V. F., Pye, H. O. T., Nenes, A., Neff, M. E., Stone, E. A., Mueller, S., Knote, C., Shaw, S. L., Zhang, Z., Gold, A., and Surratt, J. D.:

Examining the effects of anthropogenic emissions on isoprene-derived secondary organic aerosol formation during the 2013 Southern Oxidant and Aerosol Study (SOAS) at the Look Rock, Tennessee ground site, Atmos. Chem. Phys., 15, 8871-8888, 10.5194/acp-15-8871-2015, 2015.

Cai, D., Wang, X., Chen, J., and Li, X.: Molecular Characterization of Organosulfates in Highly Polluted Atmosphere Using Ultra-High-Resolution Mass Spectrometry, J. Geophys. Res. Atmos., 125, 10.1029/2019jd032253, 2020.

Chen, Y., Dombek, T., Hand, J., Zhang, Z., Gold, A., Ault, A. P., Levine, K. E., and Surratt, J. D.: Seasonal Contribution of Isoprene-Derived Organosulfates to Total Water-Soluble Fine Particulate Organic Sulfur in the United States, ACS Earth Space Chem., 5, 2419-2432, 10.1021/acsearthspacechem.1c00102, 2021.

Ding, S., Chen, Y., Devineni, S. R., Pavuluri, C. M., and Li, X.-D.: Distribution characteristics of organosulfates (OSs) in PM2.5 in Tianjin, Northern China: Quantitative analysis of total and three OS species, Sci. Total Environ., 834, 10.1016/j.scitotenv.2022.155314, 2022.

Ding, X., He, Q.-F., Shen, R.-Q., Yu, Q.-Q., Zhang, Y.-Q., Xin, J.-Y., Wen, T.-X., and Wang, X.-M.: Spatial and seasonal variations of isoprene secondary organic aerosol in China: Significant impact of biomass burning during winter, Sci. Rep., 6, 10.1038/srep20411, 2016.

Ehn, M., Kleist, E., Junninen, H., Petäjä, T., Lönn, G., Schobesberger, S., Dal Maso, M., Trimborn, A., Kulmala, M., Worsnop, D. R., Wahner, A., Wildt, J., and Mentel, T. F.: Gas phase formation of extremely oxidized pinene reaction products in chamber and ambient air, Atmos. Chem. Phys., 12, 5113-5127, 10.5194/acp-12-5113-2012, 2012.

Ehn, M., Thornton, J. A., Kleist, E., Sipila, M., Junninen, H., Pullinen, I., Springer, M., Rubach, F., Tillmann, R., Lee, B., Lopez-Hilfiker, F., Andres, S., Acir, I. H., Rissanen, M., Jokinen, T., Schobesberger, S., Kangasluoma, J., Kontkanen, J., Nieminen, T., Kurten, T., Nielsen, L. B., Jorgensen, S., Kjaergaard, H. G., Canagaratna, M., Maso, M. D., Berndt, T., Petaja, T., Wahner, A., Kerminen, V. M., Kulmala, M., Worsnop, D. R., Wildt, J., and Mentel, T. F.: A large source of low-volatility secondary organic aerosol, Nature, 506, 476-479, 10.1038/nature13032, 2014.

Glasius, M., Hansen, A. M. K., Claeys, M., Henzing, J. S., Jedynska, A. D., Kasper-Giebl, A., Kistler, M., Kristensen, K., Martinsson, J., Maenhaut, W., Nøjgaard, J. K., Spindler, G., Stenström, K. E., Swietlicki, E., Szidat, S., Simpson, D., and Yttri, K. E.: Composition and sources of carbonaceous aerosols in Northern Europe during winter, Atmos. Environ., 173, 127-141, 10.1016/j.atmosenv.2017.11.005, 2018.

Guenther, A. B., Zimmerman, P. R., Harley, P. C., Monson, R. K., and Fall, R.: Isoprene and monoterpene emission rate variability J. Geophys. Res. Atmos., 98, 12609-12617, 1993.

Guo, Y., Yan, C., Liu, Y., Qiao, X., Zheng, F., Zhang, Y., Zhou, Y., Li, C., Fan, X., Lin, Z., Feng, Z., Zhang, Y., Zheng, P., Tian, L., Nie, W., Wang, Z., Huang, D., Daellenbach, K. R., Yao, L., Dada, L., Bianchi, F., Jiang, J., Liu, Y., Kerminen, V.-M., and Kulmala, M.: Seasonal variation in oxygenated organic molecules in urban Beijing and their contribution to secondary organic aerosol, Atmos. Chem. Phys., 22, 10077-10097, 10.5194/acp-22-10077-2022, 2022.

Han, Y., Zhang, X., Li, L., Lin, Y., Zhu, C., Zhang, N., Wang, Q., and Cao, J.: Enhanced Production of Organosulfur Species during a Severe Winter Haze Episode in the Guanzhong Basin of Northwest China, Environ. Sci. Technol., 57, 8708-8718, 10.1021/acs.est.3c02914, 2023.

Hettiyadura, A. P. S., Al-Naiema, I. M., Hughes, D. D., Fang, T., and Stone, E. A.: Organosulfates in Atlanta, Georgia: anthropogenic influences on biogenic secondary organic aerosol formation, Atmos. Chem. Phys., 19, 3191-3206, 10.5194/acp-19-3191-2019, 2019.

Hettiyadura, A. P. S., Stone, E. A., Kundu, S., Baker, Z., Geddes, E., Richards, K., and Humphry, T.: Determination of atmospheric organosulfates using HILIC chromatography with MS detection, Atmos. Meas. Tech., 8, 2347-2358, 10.5194/amt-8-2347-2015, 2015.

Hettiyadura, A. P. S., Jayarathne, T., Baumann, K., Goldstein, A. H., de Gouw, J. A., Koss, A., Keutsch, F. N., Skog, K., and Stone, E. A.: Qualitative and quantitative analysis of atmospheric organosulfates in Centreville, Alabama, Atmos. Chem. Phys., 17, 1343-1359, 10.5194/acp-17-1343-2017, 2017.

Huang, L., Wang, Y., Zhao, Y., Hu, H., Yang, Y., Wang, Y., Yu, J. Z., Chen, T., Cheng, Z., Li, C., Li, Z., and Xiao, H.: Biogenic and Anthropogenic Contributions to Atmospheric Organosulfates in a Typical Megacity in Eastern China, J.

Geophys. Res. Atmos., 128, 10.1029/2023jd038848, 2023.

Huang, R.-J., Cao, J., Chen, Y., Yang, L., Shen, J., You, Q., Wang, K., Lin, C., Xu, W., Gao, B., Li, Y., Chen, Q., Hoffmann, T., O'Dowd, C. D., Bilde, M., and Glasius, M.: Organosulfates in atmospheric aerosol: synthesis and quantitative analysis of $PM_{2.5}$ from Xi'an, northwestern China, Atmos. Meas. Tech., 11, 3447-3456, 10.5194/amt-11-3447-2018, 2018.

Hughes, D. D., Christiansen, M. B., Milani, A., Vermeuel, M. P., Novak, G. A., Alwe, H. D., Dickens, A. F., Pierce, R. B., Millet, D. B., Bertram, T. H., Stanier, C. O., and Stone, E. A.: PM2.5 chemistry, organosulfates, and secondary organic aerosol during the 2017 Lake Michigan Ozone Study, Atmos. Environ., 244, 10.1016/j.atmosenv.2020.117939, 2021.

Jiang, H., Li, J., Tang, J., Cui, M., Zhao, S., Mo, Y., Tian, C., Zhang, X., Jiang, B., Liao, Y., Chen, Y., and Zhang, G.: Molecular characteristics, sources, and formation pathways of organosulfur compounds in ambient aerosol in Guangzhou, South China, Atmos. Chem. Phys., 22, 6919-6935, 10.5194/acp-22-6919-2022, 2022.

Jokinen, T., Sipila, M., Richters, S., Kerminen, V. M., Paasonen, P., Stratmann, F., Worsnop, D., Kulmala, M., Ehn, M., Herrmann, H., and Berndt, T.: Rapid autoxidation forms highly oxidized RO2 radicals in the atmosphere, Angew. Chem. Int. Ed. Engl., 53, 14596-14600, 10.1002/anie.201408566, 2014.

Kundu, S., Quraishi, T. A., Yu, G., Suarez, C., Keutsch, F. N., and Stone, E. A.: Evidence and quantitation of aromatic organosulfates in ambient aerosols in Lahore, Pakistan, Atmos. Chem. Phys., 13, 4865-4875, 10.5194/acp-13-4865-2013, 2013.

Lin, Y. H., Knipping, E. M., Edgerton, E. S., Shaw, S. L., and Surratt, J. D.: Investigating the influences of SO_2 and NH_3 levels on isoprene-derived secondary organic aerosol formation using conditional sampling approaches, Atmos. Chem. Phys., 13, 8457-8470, 10.5194/acp-13-8457-2013, 2013.

Ma, J., Ungeheuer, F., Zheng, F., Du, W., Wang, Y., Cai, J., Zhou, Y., Yan, C., Liu, Y., Kulmala, M., Daellenbach, K. R., and Vogel, A. L.: Nontarget Screening Exhibits a Seasonal Cycle of PM2.5 Organic Aerosol Composition in Beijing, Environ. Sci. Technol., 56, 7017-7028, 10.1021/acs.est.1c06905, 2022.

Nguyen, Q. T., Christensen, M. K., Cozzi, F., Zare, A., Hansen, A. M. K., Kristensen, K., Tulinius, T. E., Madsen, H. H., Christensen, J. H., Brandt, J., Massling, A., Nøjgaard, J. K., and Glasius, M.: Understanding the anthropogenic influence on formation of biogenic secondary organic aerosols in Denmark via analysis of organosulfates and related oxidation products, Atmos. Chem. Phys., 14, 8961-8981, 10.5194/acp-14-8961-2014, 2014.

Nozière, B., Ekström, S., Alsberg, T., and Holmström, S.: Radical-initiated formation of organosulfates and surfactants in atmospheric aerosols, Geophys. Res. Lett., 37, n/a-n/a, 10.1029/2009gl041683, 2010.

Olson, C. N., Galloway, M. M., Yu, G., Hedman, C. J., Lockett, M. R., Yoon, T., Stone, E. A., Smith, L. M., and Keutsch, F. N.: Hydroxycarboxylic Acid-Derived Organosulfates: Synthesis, Stability, and Quantification in Ambient Aerosol, Environ. Sci. Technol., 45, 6468-6474, 10.1021/es201039p, 2011.

Riva, M., Budisulistiorini, S. H., Zhang, Z., Gold, A., and Surratt, J. D.: Chemical characterization of secondary organic aerosol constituents from isoprene ozonolysis in the presence of acidic aerosol, Atmos. Environ., 130, 5-13, 10.1016/j.atmosenv.2015.06.027, 2016.

Riva, M., Tomaz, S., Cui, T., Lin, Y. H., Perraudin, E., Gold, A., Stone, E. A., Villenave, E., and Surratt, J. D.: Evidence for an unrecognized secondary anthropogenic source of organosulfates and sulfonates: gas-phase oxidation of polycyclic aromatic hydrocarbons in the presence of sulfate aerosol, Environ. Sci. Technol., 49, 6654-6664, 10.1021/acs.est.5b00836, 2015.

Surratt, J. D., Gómez-González, Y., Chan, A. W. H., Vermeylen, R., Shahgholi, M., Kleindienst, T. E., Edney, E. O., Offenberg, J. H., Lewandowski, M., Jaoui, M., Maenhaut, W., Claeys, M., Flagan, R. C., and Seinfeld, J. H.: Organosulfate Formation in Biogenic Secondary Organic Aerosol, J. Phys. Chem. A., 112, 8345-8378, 10.1021/jp802310p, 2008.

Tang, J., Li, J., Su, T., Han, Y., Mo, Y., Jiang, H., Cui, M., Jiang, B., Chen, Y., Tang, J., Song, J., Peng, P. a., and Zhang, G.: Molecular compositions and optical properties of dissolved brown carbon in biomass burning, coal combustion, and vehicle emission aerosols illuminated by excitation–emission matrix spectroscopy and Fourier transform ion cyclotron resonance mass spectrometry analysis, Atmos. Chem. Phys., 20, 2513-2532, 10.5194/acp-20-2513-2020, 2020.

Tao, S., Lu, X., Levac, N., Bateman, A. P., Nguyen, T. B., Bones, D. L., Nizkorodov, S.

A., Laskin, J., Laskin, A., and Yang, X.: Molecular characterization of organosulfates in organic aerosols from Shanghai and Los Angeles urban areas by nanospray-desorption electrospray ionization high-resolution mass spectrometry, Environ. Sci. Technol., 48, 10993-11001, 10.1021/es5024674, 2014.

Trostl, J., Chuang, W. K., Gordon, H., Heinritzi, M., Yan, C., Molteni, U., Ahlm, L., Frege, C., Bianchi, F., Wagner, R., Simon, M., Lehtipalo, K., Williamson, C., Craven, J. S., Duplissy, J., Adamov, A., Almeida, J., Bernhammer, A. K., Breitenlechner, M., Brilke, S., Dias, A., Ehrhart, S., Flagan, R. C., Franchin, A., Fuchs, C., Guida, R., Gysel, M., Hansel, A., Hoyle, C. R., Jokinen, T., Junninen, H., Kangasluoma, J., Keskinen, H., Kim, J., Krapf, M., Kurten, A., Laaksonen, A., Lawler, M., Leiminger, M., Mathot, S., Mohler, O., Nieminen, T., Onnela, A., Petaja, T., Piel, F. M., Miettinen, P., Rissanen, M. P., Rondo, L., Sarnela, N., Schobesberger, S., Sengupta, K., Sipila, M., Smith, J. N., Steiner, G., Tome, A., Virtanen, A., Wagner, A. C., Weingartner, E., Wimmer, D., Winkler, P. M., Ye, P., Carslaw, K. S., Curtius, J., Dommen, J., Kirkby, J., Kulmala, M., Riipinen, I., Worsnop, D. R., Donahue, N. M., and Baltensperger, U.: The role of low-volatility organic compounds in initial particle growth in the atmosphere, Nature, 533, 527-531, 10.1038/nature18271, 2016.

Wang, Y., Ren, J., Huang, X. H. H., Tong, R., and Yu, J. Z.: Synthesis of Four Monoterpene-Derived Organosulfates and Their Quantification in Atmospheric Aerosol Samples, Environ. Sci. Technol., 51, 6791-6801, 10.1021/acs.est.7b01179, 2017.

Wang, Y., Ma, Y., Kuang, B., Lin, P., Liang, Y., Huang, C., and Yu, J. Z.: Abundance of organosulfates derived from biogenic volatile organic compounds: Seasonal and spatial contrasts at four sites in China, Sci. Total Environ., 806, 10.1016/j.scitotenv.2021.151275, 2022.

Wang, Y., Zhao, Y., Wang, Y., Yu, J.-Z., Shao, J., Liu, P., Zhu, W., Cheng, Z., Li, Z., Yan, N., and Xiao, H.: Organosulfates in atmospheric aerosols in Shanghai, China: seasonal and interannual variability, origin, and formation mechanisms, Atmos. Chem. Phys., 21, 2959-2980, 10.5194/acp-21-2959-2021, 2021a.

Wang, Y., Hu, M., Wang, Y.-C., Li, X., Fang, X., Tang, R., Lu, S., Wu, Y., Guo, S., Wu, Z., Hallquist, M., and Yu, J. Z.: Comparative Study of Particulate Organosulfates in Contrasting Atmospheric Environments: Field Evidence for the Significant Influence of Anthropogenic Sulfate and NOx, Environ. Sci. Technol. Lett., 7, 787-794, 10.1021/acs.estlett.0c00550, 2020.

Wang, Y., Hu, M., Lin, P., Guo, Q., Wu, Z., Li, M., Zeng, L., Song, Y., Zeng, L., Wu, Y., Guo, S., Huang, X., and He, L.: Molecular Characterization of Nitrogen-Containing Organic Compounds in Humic-like Substances Emitted from Straw Residue Burning, Environ. Sci. Technol., 51, 5951-5961, 10.1021/acs.est.7b00248, 2017b.

Wang, Y., Zhang, Y., Li, W., Wu, G., Qi, Y., Li, S., Zhu, W., Yu, J. Z., Yu, X., Zhang, H.-H., Sun, J., Wang, W., Sheng, L., Yao, X., Gao, H., Huang, C., Ma, Y., and Zhou, Y.: Important Roles and Formation of Atmospheric Organosulfates in

Marine Organic Aerosols: Influence of Phytoplankton Emissions and Anthropogenic Pollutants, Environ. Sci. Technol., 57, 10284-10294, 10.1021/acs.est.3c01422, 2023.

Wang, Y., Hu, M., Guo, S., Wang, Y., Zheng, J., Yang, Y., Zhu, W., Tang, R., Li, X., Liu, Y., Le Breton, M., Du, Z., Shang, D., Wu, Y., Wu, Z., Song, Y., Lou, S., Hallquist, M., and Yu, J.: The secondary formation of organosulfates under interactions between biogenic emissions and anthropogenic pollutants in summer in Beijing, Atmos. Chem. Phys., 18, 10693-10713, 10.5194/acp-18-10693-2018, 2018.

Wang, Z., Ehn, M., Rissanen, M. P., Garmash, O., Quéléver, L., Xing, L., Monge-Palacios, M., Rantala, P., Donahue, N. M., Berndt, T., and Sarathy, S. M.: Efficient alkane oxidation under combustion engine and atmospheric conditions, Commun. Chem., 4, 10.1038/s42004-020-00445-3, 2021b.

Xie, Q., Su, S., Chen, J., Dai, Y., Yue, S., Su, H., Tong, H., Zhao, W., Ren, L., Xu, Y., Cao, D., Li, Y., Sun, Y., Wang, Z., Liu, C.-Q., Kawamura, K., Jiang, G., Cheng, Y., and Fu, P.: Increase of nitrooxy organosulfates in firework-related urban aerosols during Chinese New Year's Eve, Atmos. Chem. Phys., 21, 11453-11465, 10.5194/acp-21-11453-2021, 2021.

Xie, Q., Li, Y., Yue, S., Su, S., Cao, D., Xu, Y., Chen, J., Tong, H., Su, H., Cheng, Y., Zhao, W., Hu, W., Wang, Z., Yang, T., Pan, X., Sun, Y., Wang, Z., Liu, C. Q., Kawamura, K., Jiang, G., Shiraiwa, M., and Fu, P.: Increase of High Molecular Weight Organosulfate With Intensifying Urban Air Pollution in the Megacity Beijing, J. Geophys. Res.: Atmos. , 125, 10.1029/2019jd032200, 2020.

Yan, C., Nie, W., Äijälä, M., Rissanen, M. P., Canagaratna, M. R., Massoli, P., Junninen, H., Jokinen, T., Sarnela, N., Häme, S. A. K., Schobesberger, S., Canonaco, F., Yao, L., Prévôt, A. S. H., Petäjä, T., Kulmala, M., Sipilä, M., Worsnop, D. R., and Ehn, M.: Source characterization of highly oxidized multifunctional compounds in a boreal forest environment using positive matrix factorization, Atmos. Chem. Phys., 16, 12715-12731, 10.5194/acp-16-12715-2016, 2016.

Yang, T., Xu, Y., Ma, Y.-J., Wang, Y.-C., Yu, J. Z., Sun, Q.-B., Xiao, H.-W., Xiao, H.-Y., and Liu, C.-Q.: Field Evidence for Constraints of Nearly Dry and Weakly Acidic Aerosol Conditions on the Formation of Organosulfates, Environ. Sci. Technol. Lett., 10.1021/acs.estlett.4c00522, 2024.

Yang, T., Xu, Y., Ye, Q., Ma, Y.-J., Wang, Y.-C., Yu, J.-Z., Duan, Y.-S., Li, C.-X., Xiao, H.-W., Li, Z.-Y., Zhao, Y., and Xiao, H.-Y.: Spatial and diurnal variations of aerosol organosulfates in summertime Shanghai, China: potential influence of photochemical processes and anthropogenic sulfate pollution, Atmos. Chem. Phys., 23, 13433-13450, 10.5194/acp-23-13433-2023, 2023.

Yassine, M. M., Dabek-Zlotorzynska, E., Harir, M., and Schmitt-Kopplin, P.: Identification of weak and strong organic acids in atmospheric aerosols by capillary electrophoresis/mass spectrometry and ultra-high-resolution Fourier transform ion cyclotron resonance mass spectrometry, Anal. Chem., 84, 6586-6594, 10.1021/ac300798g, 2012.

Yassine, M. M., Harir, M., Dabek-Zlotorzynska, E., and Schmitt-Kopplin, P.: Structural characterization of organic aerosol using Fourier transform ion cyclotron resonance mass spectrometry: aromaticity equivalent approach, Rapid. Commun. Mass. Spectrom., 28, 2445-2454, 10.1002/rcm.7038, 2014.

Ye, Y., Zhan, H., Yu, X., Li, J., Wang, X., and Xie, Z.: Detection of organosulfates and nitrooxy-organosulfates in Arctic and Antarctic atmospheric aerosols, using ultra-high resolution FT-ICR mass spectrometry, Sci. Total Environ., 767, 10.1016/j.scitotenv.2020.144339, 2021.

Yu, Q., Ding, X., He, Q., Yang, W., Zhu, M., Li, S., Zhang, R., Shen, R., Zhang, Y., Bi, X., Wang, Y., Peng, P. a., and Wang, X.: Nationwide increase of polycyclic aromatic hydrocarbons in ultrafine particles during winter over China revealed by size-segregated measurements, Atmos. Chem. Phys., 20, 14581-14595, 10.5194/acp-20-14581-2020, 2020.